

# Body Design and Gait Generation of Chair-Type Asymmetrical Tripedal Low-rigidity Robot

Shintaro Inoue<sup>1</sup>, Kento Kawaharazuka<sup>1</sup>, Kei Okada<sup>1</sup>, and Masayuki Inaba<sup>1</sup>

**Abstract**—In this study, a chair-type asymmetric tripedal low-rigidity robot was designed based on the three-legged chair character in the movie “Suzume” and its gait was generated. Its body structure consists of three legs that are asymmetric to the body, so it cannot be easily balanced. In addition, the actuator is a servo motor that can only feed-forward rotational angle commands and the sensor can only sense the robot’s posture quaternion. In such an asymmetric and imperfect body structure, we analyzed how gait is generated in walking and stand-up motions by generating gaits with two different methods: a method using linear completion to connect the postures necessary for the gait discovered through trial and error using the actual robot, and a method using the gait generated by reinforcement learning in the simulator and reflecting it to the actual robot. Both methods were able to generate gait that realized walking and stand-up motions, and interesting gait patterns were observed, which differed depending on the method, and were confirmed on the actual robot. Our code and demonstration videos are available here: <https://github.com/shin0805/Chair-TypeAsymmetricalTripedalRobot.git>

## I. INTRODUCTION

The movie “Suzume” [1] by Makoto Shinkai was released on November 11, 2022. In the beginning of the story, a young man is enchanted into a three-legged chair. The chair is a three-legged chair with one leg missing from the original four legs, resulting in an asymmetrical and incomplete leg arrangement to the body. The legs have only two-rotational joints at the root, and there are no joints such as elbows or knees in animals. The enchanted young man in the form of a chair could not move well at first, but as the story progressed, his gait grew. Eventually, the young man had acquired a very flexible gait, running down the street and stand-up after falling down, while still in the body structure of a chair. We design this interesting body structure as a chair-type asymmetrical tripedal low-rigidity robot and generate its gait.

The robot in this study is distinctive in that it has an incomplete and asymmetric body structure, and since it has lost one leg from its originally four-legged body, it is difficult for the robot to maintain balance. Also, the actuators consist of servo motors that can only provide feed-forward angular commands with severe backlash, and only the roll, pitch, and yaw angles of the robot can be perceived, making the whole price of this robot cheaper to around \$60.

We analyze what kind of gait is generated in the robot with such a body structure by generating gait using two methods and comparing them. one is a method that generates several

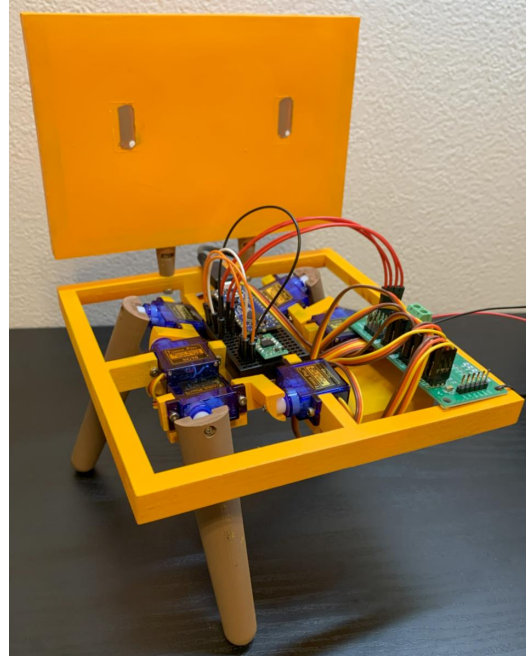


Fig. 1. Overall view of the chair-type asymmetric tripedal low-rigidity robot.

necessary postures by linear interpolation, and the other is a method that generates gait by reinforcement learning. Through a comparative analysis of these two methods, this study explores gait generation in the robot with imperfect in terms of body structures and control mechanisms.

## II. RELATED WORKS

### A. Conventional control for legged robots

In [2], the central pattern generator (CPG) was used to generate leg trajectories to make the quadruped robot walk on various uneven terrain, and in [3], the reflex circuit for walking, which is also found in cats, was implemented in the robot to achieve steady walking, but it is difficult to adapt these to the tripedal robot with an asymmetrical body structure that balances and walks. In [4], [5], the quadruped robot is controlled by model predictive control (MPC) and shows high locomotion performance in various gaits, such as walking on stairs and uneven terrain, running at a maximum of 3 m/s, and walking on 3 legs. The actuators used in the quadruped robot are brushless motors, which provide excellent controllability and backdrivability, but the actuators used in this study are low-cost servo motors with poor

<sup>1</sup> The authors are with the Department of Mechano-Informatics, Graduate School of Information Science and Technology, The University of Tokyo, 7-3-1 Hongo, Bunkyo-ku, Tokyo, 113-8656, Japan. [s-inoue, kawaharazuka, okada, inaba]@jsk.t.u-tokyo.ac.jp

controllability that is unable to provide torque control, making model-based control difficult.

### B. Reinforcement learning methods for legged robots

In the study of quadruped robot gait generation, [6] generated a gait that got up and continued walking even after falling down due to external disturbances, [7] generated a gait that adapted to various environments such as snow and gravel paths, and [8] learned to move as a goalkeeper. Also bipedal robots have acquired advanced soccer skills to compete against opponents in [9]. Compared to these studies, the robot in this study has an incomplete and asymmetrical body structure, is small (156 mm × 156 mm), and has few sensors, sensing only roll, pitch, and yaw angles. In addition, sim2real with low-cost servo motors that cost only about \$3 is required, and the output of reinforcement learning is the command position of the servo motors themselves.

### C. Robots with characteristic body structure

In [10], a tendon-driven musculoskeletal humanoid performs movements while seated on a chair with casters, with human instructions guiding gait generation. [11] explores the generation and evolution of complex body structures and corresponding gaits within a simulator, utilizing a genetic algorithm to achieve designs beyond human conception. Additionally, [12] generated gait for each body structure from one to three legs on an actual robot by reinforcement learning. [13] used a body structure of connecting trees in nature with several joints, and learned an efficient gait to go far away by reinforcement learning. [14] modeled the robot itself by randomly moving its body without knowing its own body structure, and then generated a gait that suited its body. The robot in this study differs from these robots in that it is chair-shaped and behaves in a chair-like way in generating gait, such as keeping its seat high and horizontal, and needs to keep its balance while generating gait with an imperfect and asymmetrical body structure.

## III. BODY DESIGN OF CHAIR-SHAPED ASYMMETRICAL TRIPEDAL ROBOT

### A. Design of Gimbal-Type 2-DOF Leg

The gimbal-type 2-DOF leg designed in this study is shown in Fig. 2. The rotation axes of the two servo motors intersect at the apex of the leg, allowing the leg to move forward, backward, left, and right. The servo motor that rotates the leg is fixed to a bracket, which is rotated by another servo motor. Implemented fillets on the bracket ensure each servo motor has a motion range of  $\pm 50^\circ$ . The SG-90 Micro Servo was selected, which is lightweight, space-saving, and can be driven from an Arduino.

### B. Overall Design of the Robot

The entire chair-type robot is designed by constructing three gimbal-type 2-DOF legs shown in Fig. 2. These legs are arranged to allow for six servo motors to fit within the plane of the chair's seat surface, with the ground contact points of the legs positioned near the corners of the seat rectangle.

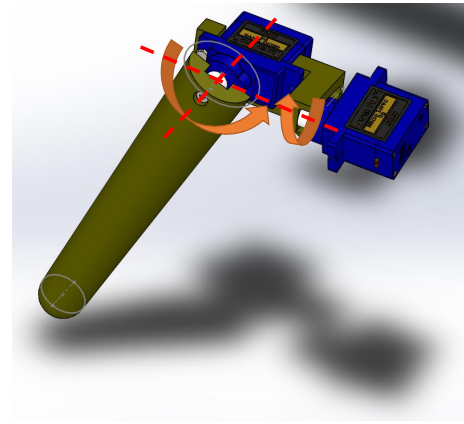


Fig. 2. Gimbal-type 2-DOF leg.

The legs' range of motion is maintained by filleting the inside of the seat surface as well as the brackets. In addition, the empty space created by the lack of one leg has a surface where a servo motor control board or microcontroller can be placed. The backrest is designed with a face similar to that of the character in the movie. The solid backrest would be difficult to stand on three legs due to the increased weight and bias, so only the frame of the backrest was designed, and a painted clear file was pasted to create the surface. Based on the above, the overall view of the chair-type asymmetric tripod low-rigidity robot designed in this study, fabricated with a 3D printer, and painted is shown in Fig. 1.

### C. System Configuration

The system configuration diagram of the robot in this study is shown in Fig. 3. The robot features an Arduino Nano Every that transmits command angles to six servo motors through the servo motor control board while receiving quaternions of its posture from the IMU. The servo motors are powered by the power supply unit via the servo motor control board. The Arduino Nano Every is wired for connection with an external PC, using ROS to exchange command angles and quaternions. This communication cycle, involving ROS, servo motors, and IMU sensor values, operates at a frequency of 10Hz. The system configuration is such that the PC executes posture planning while receiving sensor values as feedback, and the six command angles are sent to the Arduino Nano Every to realize walking and stand-up motions.

## IV. GAIT GENERATION OF CHAIR-SHAPED ASYMMETRICAL TRIPEDAL ROBOT

In this study, two methods were employed to generate the gait of a chair-type asymmetric tripod low-rigidity robot. The first method involves gait generation through connecting essential postures, while the second method involves gait generation through reinforcement learning. This chapter provides a detailed description of the steps and methods employed for each gait generation approach.

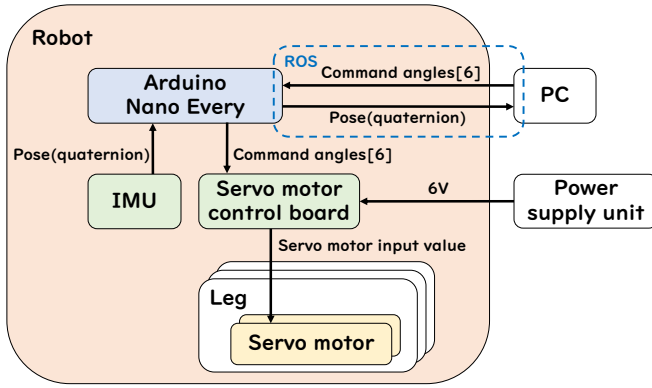


Fig. 3. System configuration.

### A. Gait Generation through Connecting Essential Posture

The posture of the robot is determined by the angles of its six servo motors, which are then represented as a single point in a six-dimensional space. To generate gait, the essential postures required for the motion process are discovered through experimentation with the actual robot. The robot's gait is generated by transitioning between these postures using linear interpolation. A posture  $S$  denotes a 6-dimensional vector containing the angles of the six servo motors.

$$S = [\theta_0 \ \theta_1 \ \theta_2 \ \theta_3 \ \theta_4 \ \theta_5]^T$$

The process of connecting essential postures using linear interpolation can be expressed as follows: when moving from one posture  $S_i$  to the subsequent posture  $S_{i+1}$ , the interpolation posture  $s$  is employed.

$$\begin{aligned} [S_i \ S_{i+1}] \begin{bmatrix} 1 & \frac{n}{n+1} & \frac{n-1}{n+1} & \dots & \frac{1}{n+1} & 0 \\ 0 & \frac{1}{n+1} & \frac{2}{n+1} & \dots & \frac{n}{n+1} & 1 \end{bmatrix} \\ = [S_i \ s_1 \ s_2 \ \dots \ s_n \ S_{i+1}] \end{aligned}$$

Using these expressions, the following concrete steps are taken

- 1) Determine the initial posture  $S_0$ .
- 2) Determine the end posture  $S_f$ .
- 3) Tentatively determine the essential posture  $S_i$  manually in the connecting essential postures process.
- 4) Transition and operate the actual robot posture from  $S_0$  to  $S_f$  via  $S_i$  by linear interpolation in  $n_i$  steps.
- 5) Modify  $n_i$ , or modify / add / delete  $S_i$  so that the motion is achieved.
- 6) Repeat (4) and (5) until the motion is achieved.

$\theta_j$  ( $j = 0, 1, 2, 3, 4, 5$ ) corresponds to each servo motor as in Fig. 4.  $\theta_j = 90^\circ$  in the posture where all three legs are vertical to the ground.

1) *Walking Motion*: The postures and the number of linear interpolations found in the walking motion are shown in Fig. 5 and Table I. This walking motion sets a standing posture for the initial and final postures, and puts the front foot forward at  $S_1$ , the left rear foot forward at  $S_2$ , and the right rear foot forward at  $S_3$ . By repeating these posture transitions, the robot walks.

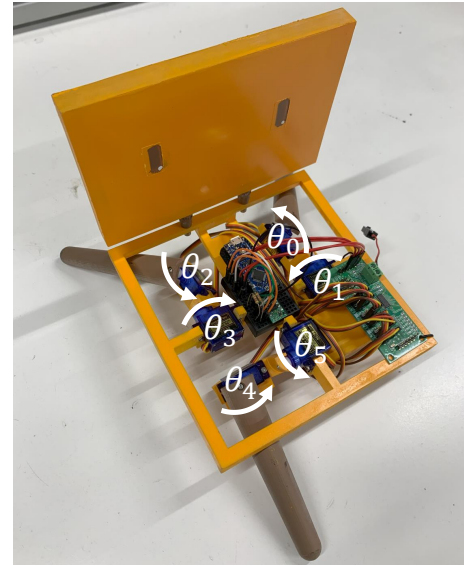


Fig. 4. Correspondence between the servo motors and  $\theta_j$ .

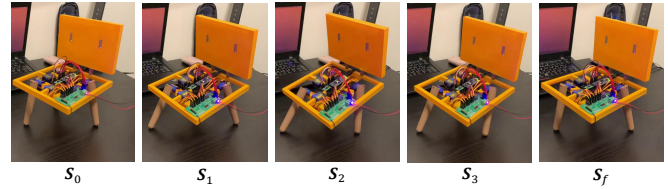


Fig. 5. Walking motion by connecting essential posture.

2) *Stand-up Motion*: The posture and the number of linear interpolations found in the stand-up motion are shown in Fig. 6 and Table II. In this stand-up motion, the initial posture is set with the robot's right side surface on the ground, and the end posture is set with the robot in a standing posture. At  $S_1$ , the robot tilts its seat by extending its legs in the opposite direction to that in which the seat is stand-up, and at  $S_2$ , the robot turns its seat upward by folding its legs and using their reaction. Then, at  $S_3$ , the legs move outward to the end posture.

### B. Gait Generation through Reinforcement Learning

The second method of gait generation is through reinforcement learning. In this study, walking and stand-up motions are generated by the reinforcement learning algorithm Prox-

TABLE I  
POSTURE AND THE NUMBER OF LINEAR INTERPOLATIONS IN WALKING MOTION.

	Posture	Steps
$S_0$	$[90^\circ \ 80^\circ \ 90^\circ \ 100^\circ \ 90^\circ \ 100^\circ]^T$	0
$S_1$	$[90^\circ \ 80^\circ \ 90^\circ \ 100^\circ \ 90^\circ \ 140^\circ]^T$	0
$S_2$	$[70^\circ \ 80^\circ \ 90^\circ \ 100^\circ \ 90^\circ \ 140^\circ]^T$	0
$S_3$	$[70^\circ \ 80^\circ \ 110^\circ \ 100^\circ \ 90^\circ \ 140^\circ]^T$	6
$S_f$	$[90^\circ \ 80^\circ \ 90^\circ \ 100^\circ \ 90^\circ \ 100^\circ]^T$	

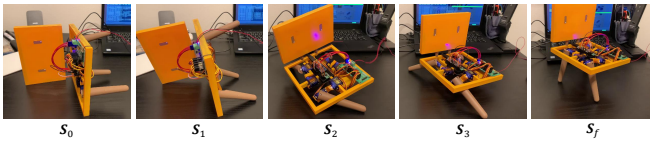


Fig. 6. Stand-up motion by posture transition.

TABLE II

POSTURE AND THE NUMBER OF LINEAR INTERPOLATIONS IN STAND-UP MOTION.

	Posture	Steps
$S_0$	$[90^\circ \ 80^\circ \ 90^\circ \ 100^\circ \ 90^\circ \ 100^\circ]^\top$	8
$S_1$	$[90^\circ \ 80^\circ \ 90^\circ \ 140^\circ \ 40^\circ \ 90^\circ]^\top$	0
$S_2$	$[130^\circ \ 80^\circ \ 40^\circ \ 90^\circ \ 150^\circ \ 140^\circ]^\top$	38
$S_3$	$[130^\circ \ 40^\circ \ 50^\circ \ 140^\circ \ 90^\circ \ 140^\circ]^\top$	28
$S_f$	$[90^\circ \ 80^\circ \ 90^\circ \ 100^\circ \ 90^\circ \ 100^\circ]^\top$	

imal Policy Optimization (PPO) [15] in the physical simulation environment called Isaac Gym [16]. The robot model used in the simulation is represented by MJCF (MuJoCo XML File), a modeling file for the MuJoCo simulator [17]. The model includes legs, brackets, seat, backrest, and servo motor joints, as shown in Fig. 7. The actuator parameters in MuJoCo were hand-tuned so that the behavior was close to reality by moving the leg in the simulation while viewing the MuJoCo viewer after the theoretical values were set.



Fig. 7. Robot model used in reinforcement learning simulation.

For reinforcement learning, the action  $\mathbf{a} \in \mathbb{R}^6$  is the command angle for 6 servo motors, and the observation  $\mathbf{s} \in \mathbb{R}^{40}$  is the combination of the quaternion output by IMU and the servo motor command angle for four periods. In other words, the next action is determined from the time series data for the last 4 control cycles of the posture (quaternion) and the servo motor command angle. Reward and reset conditions are defined separately for walking and stand-up motions. The result of training is an inference model whose input is an observation  $\mathbf{s}$  and output is an action  $\mathbf{a}$ .

The IMU sensor values and the servo motor command angle in the actual robot are input to the inference model

in the same format as during learning, and the servo motor command angle, which is the next action, is obtained. By sending this command angle to the actual robot, what is learned in the simulation is reflected in the actual robot.

The following variables are introduced to explain the rewards and reset conditions.

- $\mathbf{p} = [x \ y \ z]^\top$   
: Current coordinates of the robot (center of the seat)
- $\mathbf{q} = [q_x \ q_y \ q_z \ q_w]^\top$   
: Posture of the seat
- $\mathbf{R}_q$   
: Rotation matrix of  $\mathbf{q}$
- $\mathbf{p}_{\text{target}} = [10 \ 0 \ 0]^\top$   
: Target coordinates / m
- $dt = 0.1$   
: Period of simulator / s
- $\mathbf{e}_x = [1 \ 0 \ 0]^\top$   
: Forward unit vector
- $\mathbf{e}_z = [0 \ 0 \ 1]^\top$   
: Vertical upward unit vector
- $\mathbf{a} = [\theta_0 \ \theta_1 \ \theta_2 \ \theta_3 \ \theta_4 \ \theta_5]^\top$   
: Servo motor command angle
- $\boldsymbol{\omega} = [\omega_0 \ \omega_1 \ \omega_2 \ \omega_3 \ \omega_4 \ \omega_5]^\top$   
: Servo motor angular velocity
- $u_{\text{prj}} = |\mathbf{R}_q \mathbf{e}_z|_z$   
: z component of the seat upward unit vector

1) *Walking Motion*: The rewards and their weights are summarized in Table IV and the reset conditions are summarized in Table III. Rewards are designed to be highest when moving forward while keeping the seat horizontal and high. However, a gait in which the robot moves forward while rubbing its back against the ground was learned as a case in which the reward was high even though the robot was not in such a state. The reset conditions were set to prevent such a gait from being learned. After training about 100 epochs of 131072 agents simultaneously, about 30 epochs of additional training were conducted with noise randomly added to physical parameters, sensor values and action values. The walking behavior on the simulator after training is shown in Fig. 8.

TABLE III

RESET CONDITIONS FOR WALKING MOTION.

Reset	Condition
max episode	When the episode exceeds 350.
tilt	When $\ \mathbf{q} - [0, 0, 0, 1]^\top\  > 0.7$
ground	When any corner of the seat surface contacts the ground.
height	When the seat height becomes lower than 5 mm.

2) *Stand-up Motion*: The rewards and their weights are summarized in Table VI and the reset conditions are summarized in Table V. The most reward is given to the agent that turns the seat face up, but this is not enough to solve the problem of the agent that turns the seat face up with each leg folded inward and cannot stand up from there. The problem is solved by rewarding the outward spreading of

TABLE IV  
REWARDS AND WEIGHTS IN WALKING MOTION.

Reward	Description and purpose	Weight
progress	$P - P_{\text{pre}}$ where $P = -\frac{\ \mathbf{p}_{\text{target}} - \mathbf{p}\ }{dt}$ and $P_{\text{pre}}$ is the previous cycle's $P$ Reward for moving forward.	30
height	$\min\left\{1, \frac{ \mathbf{p} _z}{0.08}\right\}$ Reward for high seat height.	20
up	$\min\left\{1, \frac{u_{\text{prj}}}{0.93}\right\}$ Reward for a vertically upward seat.	5
heading	$\min\left\{1, \frac{1}{0.8} R_q e_x \cdot \frac{\mathbf{p}_{\text{target}} - \mathbf{p}}{\ \mathbf{p}_{\text{target}} - \mathbf{p}\ }\right\}$ Reward for the direction in which one is moving toward the target point.	2
alive	Reward for not being reset. Unless it is reset, this gives a constant value.	1
death	The reward is given when the reset condition other than the max episode is satisfied. This value overwrites the previous rewards.	-1
action	$\ \mathbf{a} - \mathbf{a}_{\text{pre}}\ ^2$ where $\mathbf{a}_{\text{pre}}$ is the previous cycle's $\mathbf{a}$ Penalty for the absolute value of the difference of the command angle from the previous cycle.	-2
vel	$\left\ \frac{\boldsymbol{\omega}}{\boldsymbol{\omega}_{\text{max}} - \boldsymbol{\omega}_{\text{tol}}}\right\ ^2$ where $\boldsymbol{\omega}_{\text{max}} = 10.472$ , $\boldsymbol{\omega}_{\text{tol}} = 1$ Penalty for the magnitude of the joint angular velocity.	-2

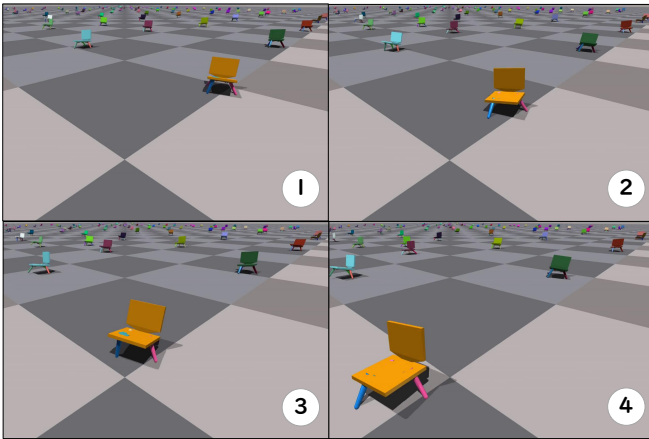


Fig. 8. Walking motion on the simulator.

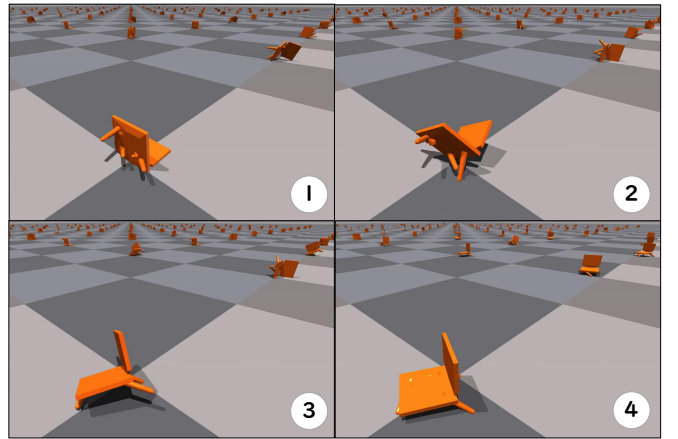


Fig. 9. Stand-up motion on the simulator.

each leg and resetting the agent that cannot stand up and whose seat surface has turned upward. 131072 agents were simultaneously trained for approximately 250 epochs. Three initial postures were prepared for the robot at the beginning of training: right side, left side, and back on the ground, and the robot learned to stand-up from these postures at once. The rise motion on the simulator after learning is shown in Fig. 9.

TABLE V  
RESET CONDITIONS IN THE STAND-UP MOTION.

Reset	Condition
max episode	When the episode exceeds 350.
flip	When $u_{\text{prj}} < -0.7$
fold	When $0.6 < u_{\text{prj}}$ and $\max\{\ [\theta_0, \theta_1, \theta_3, \theta_5]^T - \mathbf{a}_{\text{expand}}\ _{\infty}\} > 1$

## V. EXPERIMENTS

### A. Experiment Overview and Environment

In this experiment, the  $x, y$  coordinates, roll angle, pitch angle, and yaw angle of the robot are measured, and the command angles of the servo motors in the walking and stand-up motions are measured over time to analyze the gait by connecting essential postures and the gait by the reinforcement learning method. During walking, the robot moves forward along the  $x$ -axis, and during stand-up motion, the robot stands up from a state in which the side of the robot's seat is on the ground. The experimental environment is shown in Fig. 15. For evaluation purposes, the robot's  $x, y$  coordinates are measured using the AR marker, and the roll, pitch, yaw angles are measured using the IMU .

TABLE VI  
REWARDS AND WEIGHTS IN THE STAND-UP MOTION.

Reward	Description and purpose	Weight
up	$\min\{1, \exp\{2(u_{prj} - 1)\}\}$ Reward for the seat being vertically upward.	250
standing	$\begin{cases} \frac{1}{2 \arcsin(\min\{1, \ \mathbf{a} - \mathbf{a}_{stand}\ _4\})  + 0.1} & (u_{prj} > 0.85) \\ 0 & (\text{otherwise}) \end{cases}$ where $\mathbf{a}_{stand} = [-0.1745, 0, -0.1745, 0, 0.1745, 0]^\top$ Reward for the proximity of each joint angle to the standing posture.	100
spreading	$\begin{cases} \frac{1}{2 \arcsin(\min\{1, \ [\theta_0, \theta_1, \theta_3, \theta_5]^\top - \mathbf{a}_{expand}\ _4\})  + 0.1} & (u_{prj} > 0.2) \\ 0 & (\text{otherwise}) \end{cases}$ where $\mathbf{a}_{expand} = [-1, -1, 1, -1]^\top$ Reward for each leg not being folded inward during the process of seat upward.	50
death	The reward is given when the reset condition other than the max episode is satisfied. This value overwrites the previous rewards.	-1
action	$\ \mathbf{a} - \mathbf{a}_{pre}\ ^2$ where $\mathbf{a}_{pre}$ is the previous cycle's $\mathbf{a}$ Penalty for the absolute value of the difference of the command angle from the previous cycle.	-2

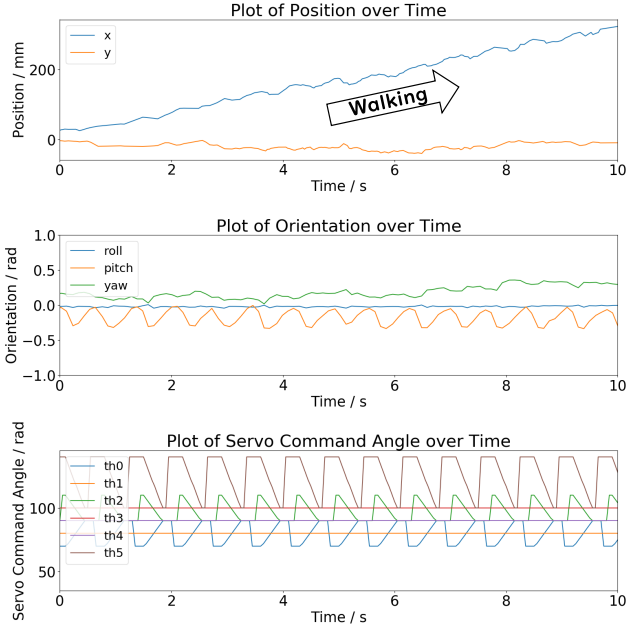


Fig. 10. Result of walking motion by connecting essential postures.

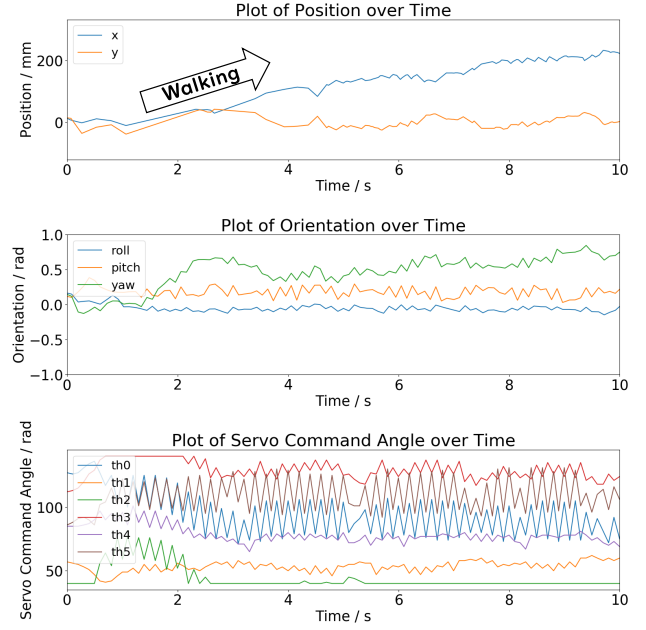


Fig. 11. Results of walking motion by reinforcement learning.

## B. Walking Motion

Fig. 10 is the result of walking motion by connecting essential postures. The walking motion is realized by repeatedly transitioning from the posture  $S_0$  to  $S_f$ . Since the posture transition is a feed-forward command, the command angle shows always the same pattern regardless of the robot's position or posture. The  $x, y$  coordinates of the graph show that the robot is moving forward at a constant speed. The pitch angle shows that the robot is swinging its posture in the pitch direction at a constant period.

Fig. 11 is the result of the walking motion by reinforcement learning. The  $x, y$  coordinates of the graph show that the robot is moving forward, but its speed is not constant.

The robot moves forward significantly from time 2 to 4 seconds, while it hardly moves forward at time 8 to 10 seconds. The yaw angle shows that the robot is moving forward while looking at  $35^\circ$  diagonally to the left. The gait by reinforcement learning was a gait in which the entire body was shaken up and down by vibrating the joint angles. When the body was about to move in the upward direction by the vibration, the gait was to move forward by kicking the ground with the legs. The pitch angle was always upward and the amplitude of the vibration was smaller than that of walking motion by connecting essential postures.

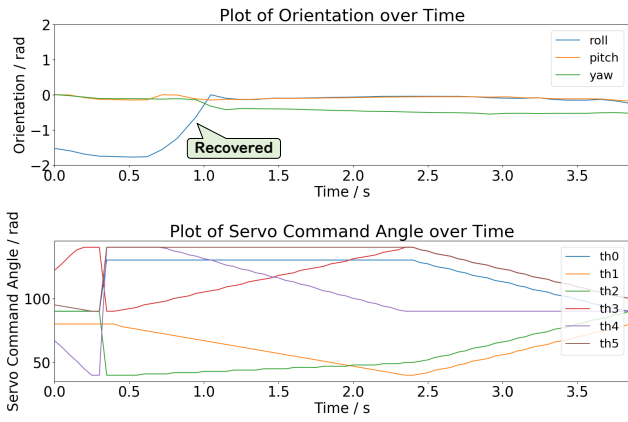


Fig. 12. The result of stand-up by connecting essential postures.

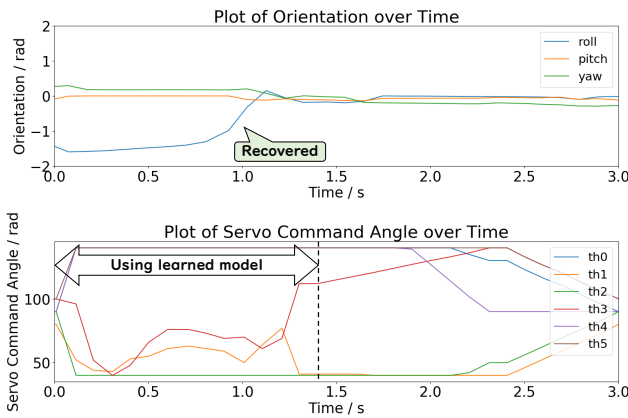


Fig. 13. Result of stand-up by reinforcement learning.

### C. Stand-up Motion

Fig. 12 is the result of a stand-up motion by connecting essential postures. The robot is performing the action of stand-up from the position where the right side of the seat is on the ground. The roll angle shows that the robot is tilted further than  $90^\circ$  and then rises to  $0^\circ$ . The servo motor command angle shows that the robot is pushing and tilting its body with its legs and then quickly releasing it to raise its posture.

Fig. 13 shows the result of stand-up motion by reinforcement learning. The movement from the right side of the seat to stand-up is the result of reinforcement learning, and the movements after that are pre-defined movements. As with the stand-up motion by connecting essential postures, the seat was tilted backward and then started to stand-up. In addition, the  $\theta_1$  and  $\theta_3$  change significantly from 1 second to 1.5 seconds.  $\theta_3$  is the leg that kicks the ground, while  $\theta_1$  is the upper leg of the pair. The large change in  $\theta_1$  generates inertial force in the direction of stand-up, which is also utilized to realize the stand-up motion.

As described in the Section IV-B.2, the initial posture of the robot at the beginning of the learning process is not only

the robot's right side of the seat on the ground, but also the left side and the back of the robot. Therefore, the robot can rise from various postures. This is shown in Fig. 14, which shows the robot in a standing posture that is repeatedly knocked over by a hand from the outside, and then stand-up from that posture. The robot was knocked over in the order of right side, back, left side, and right side, and it can be seen that the robot rises from any of the postures. Although the yaw angle was included in the observation, it was not involved in the rewards, so the robot took various postures with no restriction on the yaw angle.

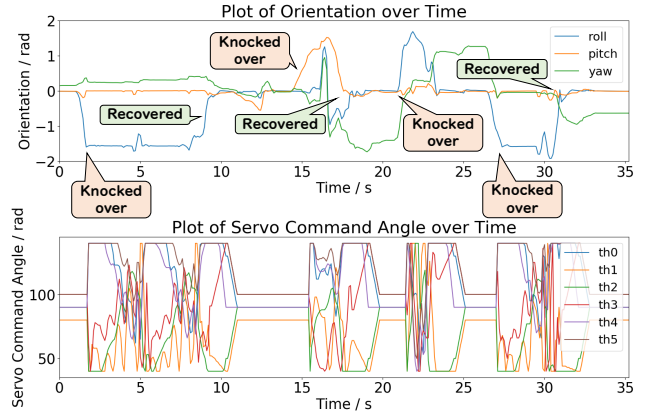


Fig. 14. Stand-up from various postures by reinforcement learning.

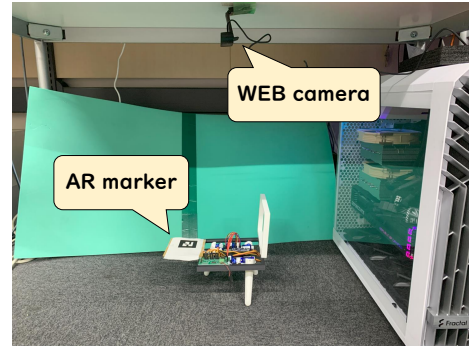


Fig. 15. Experimental environment.

## VI. DISCUSSION

The walking motion by connecting essential postures, involves the robot moving forward by putting out its 3 legs one by one in sequence. However, walking motion by reinforcement learning was the robot moving forward on three legs, vibrating the robot's entire body. The preference for vibrating motion in the walking motion by reinforcement learning can be attributed to the consideration of falling during walking. In the walking style where the robot moves one leg at a time, it momentarily relies on two legs to support its body, then proceeds forward through a falling motion. When raising one of the legs, or when the leg that has been lifted out re-enters the ground, the robot may tilt and fall,

depending on the position of the legs. In contrast, the gait of reinforcement learning is to move forward with the three legs spread wide and stability maintained. Agents that have a falling gait are reset and not rewarded during learning, so they will have a non-falling gait after learning. Consequently, gait with reinforcement learning has a lower risk of falling than gait by connecting essential postures. Moreover, the pitch angle of the robot in walking by connecting essential postures remains approximately  $0^\circ$ , while it is approximately  $35^\circ$  in walking by reinforcement learning. This difference in pitch angles can be attributed to the asymmetry of the robot's body structure. In the case of the reinforcement learning approach, the robot moves forward while facing approximately  $35^\circ$ , aligning the three legs symmetrically with its trajectory, effectively compensating for the body's asymmetry.

Regarding the stand-up motion, both the connecting essential postures and reinforcement learning approaches utilize a reaction by tilting the seat in the opposite direction of stand-up. Additionally, in the reinforcement learning approach, a distinct behavior emerges during stand-up movements: the robot attempts to stand-up by using the inertial force generated from swinging its legs. Furthermore, the robot achieves successful stand-up from various initial postures, such as the right side, back, or left side of the seat on the ground, guided by feedback from the IMU sensor within the inference model. It is thought that the robot has learned which leg should be kicked where in a certain posture to lead to the stand-up motion.

In addition, for both movements, the reset conditions play a crucial role in the gait generation within the reinforcement learning process. Some movements resulted in the robot dragging its back and seat on the ground while moving forward during the walking motion. Other agents involved the seat facing upward but not fully stand-up. Such rewarding but unexpected movements could not be addressed by adjusting the reward's content or weight. The reset conditions effectively narrow the gait space for a robot with the incomplete and asymmetrical body structure, promoting the generation of the required gait. Conversely, relaxing the reset conditions could lead to increased chances of generating unexpected gaits.

## VII. CONCLUSION

In this study, we designed a chair-type tripedal low-rigidity robot with an asymmetric and imperfect body structure, and generated its gait using two methods: connecting essential postures method and a reinforcement learning method. Both methods succeeded in generating walking and stand-up motions. In the walking motion, the gait generated by the reinforcement learning method was more stable than that by the connecting essential postures method. In the stand-up motion, both methods showed similar motions, but the gait with reinforcement learning potentially included sensor feedback and succeeded in stand-up motions from various postures. Even for robots with asymmetrical and imperfect body structures, it is possible to generate a gait

by finding and connecting postures through trial and error or by reinforcement learning. While the connecting essential postures method can quickly produce a gait specific to the desired movement, the reinforcement learning method includes robust movements that take into account the robot's body structure, although there are difficulties in adjusting the conditions and parameters during learning.

## REFERENCES

- [1] M. Shinkai, "Suzume," [Film], 2022.
- [2] C. Liu, Q. Chen, and D. Wang, "Cpg-inspired workspace trajectory generation and adaptive locomotion control for quadruped robots," *IEEE Transactions on Systems, Man, and Cybernetics, Part B (Cybernetics)*, vol. 41, no. 3, pp. 867–880, 2011.
- [3] T. Tanikawa, Y. Masuda, and M. Ishikawa, "A reciprocal excitatory reflex between extensors reproduces the prolongation of stance phase in walking cats: Analysis on a robotic platform," *Frontiers in Neuro-robotics*, vol. 15, p. 636864, 2021.
- [4] G. Bledt, M. J. Powell, B. Katz, J. Di Carlo, P. M. Wensing, and S. Kim, "Mit cheetah 3: Design and control of a robust, dynamic quadruped robot," in *2018 IEEE/RSJ International Conference on Intelligent Robots and Systems (IROS)*. IEEE, 2018, pp. 2245–2252.
- [5] J. Di Carlo, P. M. Wensing, B. Katz, G. Bledt, and S. Kim, "Dynamic locomotion in the mit cheetah 3 through convex model-predictive control," in *2018 IEEE/RSJ international conference on intelligent robots and systems (IROS)*. IEEE, 2018, pp. 1–9.
- [6] J. Lee, J. Hwangbo, and M. Hutter, "Robust recovery controller for a quadrupedal robot using deep reinforcement learning," *arXiv preprint arXiv:1901.07517*, 2019.
- [7] J. Lee, J. Hwangbo, L. Wellhausen, V. Koltun, and M. Hutter, "Learning quadrupedal locomotion over challenging terrain," *Science robotics*, vol. 5, no. 47, p. eabc5986, 2020.
- [8] X. Huang, Z. Li, Y. Xiang, Y. Ni, Y. Chi, Y. Li, L. Yang, X. B. Peng, and K. Sreenath, "Creating a dynamic quadrupedal robotic goalkeeper with reinforcement learning," *arXiv preprint arXiv:2210.04435*, 2022.
- [9] T. Haarnoja, B. Moran, G. Lever, S. H. Huang, D. Tirumala, M. Wulfmeier, J. Humplik, S. Tunyasuvunakool, N. Y. Siegel, R. Hafner, *et al.*, "Learning agile soccer skills for a bipedal robot with deep reinforcement learning," *arXiv preprint arXiv:2304.13653*, 2023.
- [10] K. Kawaharazuka, K. Okada, and M. Inaba, "Realization of seated walk by a musculoskeletal humanoid with buttock-contact sensors from human constrained teaching," in *2022 IEEE/RSJ International Conference on Intelligent Robots and Systems (IROS)*. IEEE, 2022, pp. 5774–5780.
- [11] K. Sims, "Evolving Virtual Creatures," in *Proceedings of the 21st Annual Conference on Computer Graphics and Interactive Techniques*, 1994, pp. 15–22.
- [12] S. Ha, J. Kim, and K. Yamane, "Automated deep reinforcement learning environment for hardware of a modular legged robot," in *2018 15th international conference on ubiquitous robots (UR)*. IEEE, 2018, pp. 348–354.
- [13] M. Azumi, K. Ayaka, Y. Hironori, H. Jun, N. Jason, and S. Shunta, "Improvised robotic design with found objects," in *Proc. 3rd Conf. NeurIPS Workshop Mach. Learn. Creativity Des.*, 2018.
- [14] J. Bongard, V. Zykov, and H. Lipson, "Resilient machines through continuous self-modeling," *Science*, vol. 314, no. 5802, pp. 1118–1121, 2006.
- [15] J. Schulman, F. Wolski, P. Dhariwal, A. Radford, and O. Klimov, "Proximal policy optimization algorithms," *arXiv preprint arXiv:1707.06347*, 2017.
- [16] V. Makoviychuk, L. Wawrzyniak, Y. Guo, M. Lu, K. Storey, M. Macklin, D. Hoeller, N. Rudin, A. Allshire, A. Handa, *et al.*, "Isaac gym: High performance gpu-based physics simulation for robot learning," *arXiv preprint arXiv:2108.10470*, 2021.
- [17] E. Todorov, T. Erez, and Y. Tassa, "MuJoCo: A physics engine for model-based control," in *Proceedings of the 2012 IEEE/RSJ International Conference on Intelligent Robots and Systems*, 2012, pp. 5026–5033.